CrossMark

ORIGINAL ARTICLE

Evaluation of the organic matter sources and $\delta^{13}C$ composition of individual alkanes for the baseline assessment of hydrocarbons in a pristine area from Amazon region, Brazil

Marcela Moreno Berg[1] · Celeste Yara dos Santos Siqueira[1,2] · Luiz Landau[1] ·
Fernando Pellon de Miranda[1] · Thamires Silva Mello[2] · Francisco Radler de Aquino Neto[2]

Abstract This study focuses on the surroundings of the Urucu oil and gas province and the adjoining Solimões terminal in the Amazon region of Brazil, which is of great global importance due to its biodiversity richness and freshwater resources. There are few results related to aliphatic hydrocarbons and polycyclic aromatic hydrocarbons (PAHs), and there are no results for individual stable isotopic compositions ($\delta^{13}C$) in the studied region. Results showed a distribution of *n*-alkanes that is characteristic of a major input from higher plants. Furthermore, $\delta^{13}C$ values of individual *n*-alkanes varied between −35.0 and −23.1 ‰, suggesting a dominance of ^{12}C-enriched *n*-alkanes indicative of an origin from lacustrine algae. The levels of some PAHs (4.64–31.70 ng g^{-1}) which are classified as priority pollutants by the United States Environmental Protection Agency (US-EPA) and perylene (biogenic PAH) were measured in surface sediments to identify pollution sources and determine baseline data looking for future management strategies. The majority of the compounds present in the samples from Coari Lake and the Solimões River are of biogenic origin. However, a minor anthropogenic contribution of aromatic hydrocarbons derived from biomass burning (anthracene, phenanthrene, fluoranthene, pyrene, chrysene, benzo[b]fluoranthene and benzo[k]fluoranthene) was detected. No petrogenic contribution was found in the samples.

Keywords Aliphatic hydrocarbons · Polycyclic aromatic hydrocarbons · $\delta^{13}C$ · Amazon

Introduction

The Amazon region of Brazil constitutes one of the last pristine ecosystems of the planet, with a low degradation degree and sparse rural populations that survive mostly on natural resources and subsistence agriculture (Freitas and Rivas 2003). Activities of the petroleum industry in the study area began in October 1986 with the discovery of the Urucu oil and gas province by Petrobras (the Brazilian national oil company). Implanted transportation infrastructure includes a pipeline leading to the Solimões Terminal (TESOL), which is situated on the right margin of the Solimões River near the Coari Lake mouth. From this terminal, the oil is taken by a tanker to the Isaac Sabbá Refinery (REMAN), located 600 km downriver in the Manaus city, the capital of the Amazon State. Urucu's daily production is about 55,000 barrels of oil and 1500 tons of liquefied petroleum gas (LPG). However, operations present an inherent environmental risk, such as oil spills into the aquatic environment (Almeida and Souza 2008). The PIATAM Project was conceived by Petrobras and local academia as an attempt to assess the potential risks stated above. This is an extensive environmental research initiative created to monitor the petroleum production and transportation from Urucu to Manaus. Among other scientific goals, PIATAM aims to consolidate socio-

✉ Marcela Moreno Berg
  marcelaberg.jf@hotmail.com

1 Laboratório de Métodos Computacionais em Engenharia, Instituto Alberto Luiz Coimbra de Pós-Graduação e Pesquisa de Engenharia, Universidade Federal do Rio de Janeiro, 21941-909 Rio de Janeiro, Brazil

2 Instituto de Química, Universidade Federal do Rio de Janeiro, 21941-909 Rio de Janeiro, Brazil

Springer

environmental information in a digital database (Castro et al. 2008). Indeed, there are no reported cases of oil spill in the region. However, it is important to have a baseline of information that will be valuable for future environmental monitoring programs.

Knowledge of the factors governing the spatial and temporal variations of the particle size and composition is of primary importance in reaching an understanding of sediment–contaminant correlations (Nehyba et al. 2010). Composition varies with grain size due to several factors (varied sources contributing mineralogically and texturally distinct grain sizes, processes of mechanical and chemical weathering, sorting of grains with a distinct composition during transport) (Whitmore et al. 2004). A number of authors have evaluated the relationship between sediment grain size to modal composition and geochemistry often with respect to anthropogenic factors (Cox and Lowe 1996; Decker and Helmond 1985; Nesbitt et al. 1996; Roser and Korsch 1986; Stone and Walling 1996; Whitmore et al. 2004; Nehyba et al. 2010).

There are few published results in the investigated site referring to aliphatic hydrocarbons (AHs) and polycyclic aromatic hydrocarbons (PAHs) (Laflamme and Hites 1978; Elias et al. 2000; Boot et al. 2006). In addition, to the best of our knowledge, there are no results regarding individual n-alkanes stable isotopic compositions ($\delta^{13}C$) determined in the Amazon region. Hydrocarbons are generally a robust record of the sedimentary organic matter origin (Meyers 2003). Hydrocarbons may also have several sources, such as terrestrial plant waxes, marine phytoplankton and bacteria, as well as biomass combustion and diagenetic transformation of biogenic precursors (Gogou et al. 2000). There are also biogenic aliphatic hydrocarbons such as hopanes which are relatively specific to the biota which produces them. Planktonic and benthic organisms synthesize hydrocarbons clearly distinguishable from the hydrocarbons found in the surface waxes of higher plants (Gomes and Azevedo 2003).

The odd-to-even-number n-alkane concentration ratios from C_{25} to C_{34}, commonly referred to as the carbon preference index (CPI), have been used to suggest their sources (Peters et al. 2005). Since n-alkanes present non-unique chain length signatures, the carbon isotopic signature can be used to better distinguish among possible sources (Sikes et al. 2009).

Polycyclic aromatic hydrocarbons (PAHs) have received special attention because these compounds may exhibit mutagenic and carcinogenic effects. PAHs have been recognized as hazardous environmental chemicals. Aside from anthropogenic sources, hydrocarbons have also several natural ones, such as terrestrial plant waxes, marine phytoplankton and bacteria, biomass combustion and diagenetic transformation of biogenic precursors (Gogou et al. 2000).

The present study evaluates these anthropogenic activity impacts in the Coari Lake and Solimões River and determines the sedimentary organic matter origins. A large number of individual compounds were measured for each compound group to detail compositional fingerprints reflecting the current pollution status and organic matter sources. The organic markers such as n-alkanes, hopanes and polycyclic aromatic hydrocarbons were evaluated to identify pollution sources, understand their contamination status and determine data for future applications.

Experimental

Study area

The study area is located in the Amazonas State central region, near the Coari municipality, Northern Brazil (Fig. 1). Coari has about 85,000 inhabitants of which approximately 50,000 live in the metropolitan center and 35,000 are spread among the 85 riverside communities under its jurisdiction (Matos et al. 2011). It is the fifth most populous Amazonas State municipality. Furthermore, oil exploration is the city's main business (IBGE 2015).

The sediment samples were collected based on the previous studies in the region that simulated a 1000 m^3 of soft oil spilled (42°API), in the Solimões River. This simulation concluded that the oil would enter the Coari Lake (Almeida and Souza 2010). Popcorn was used to simulate the oil spill due to its similar pattern of dispersion in the water surface.

Sample collection

Superficial samples were collected at 10 sites in November 2012 (Fig. 1). In Solimões River, samples were taken in front of TESOL (T2), before (T1) and after (T3). In Coari Lake, samples (S4, S5, S6, S7, S8, S9 and S10) were taken in the inlet to the lake. Sediment sampling was performed using a stainless steel van-Veen grab. The surface layer of sediment was carefully subsampled and transferred to aluminum containers, previously decontaminated at 450 °C.

Grain size analysis and total organic carbon

Sediment grain size was determined with a particle laser CILAS® 1004 analyzer and granulometric distribution curves established with the statistical program Gradstat 4.0. Prior to analyses, the samples were treated sequentially for 2 weeks with 10 % H_2O_2, centrifuged and washed with distilled water to eliminate organics. Prior to being injected
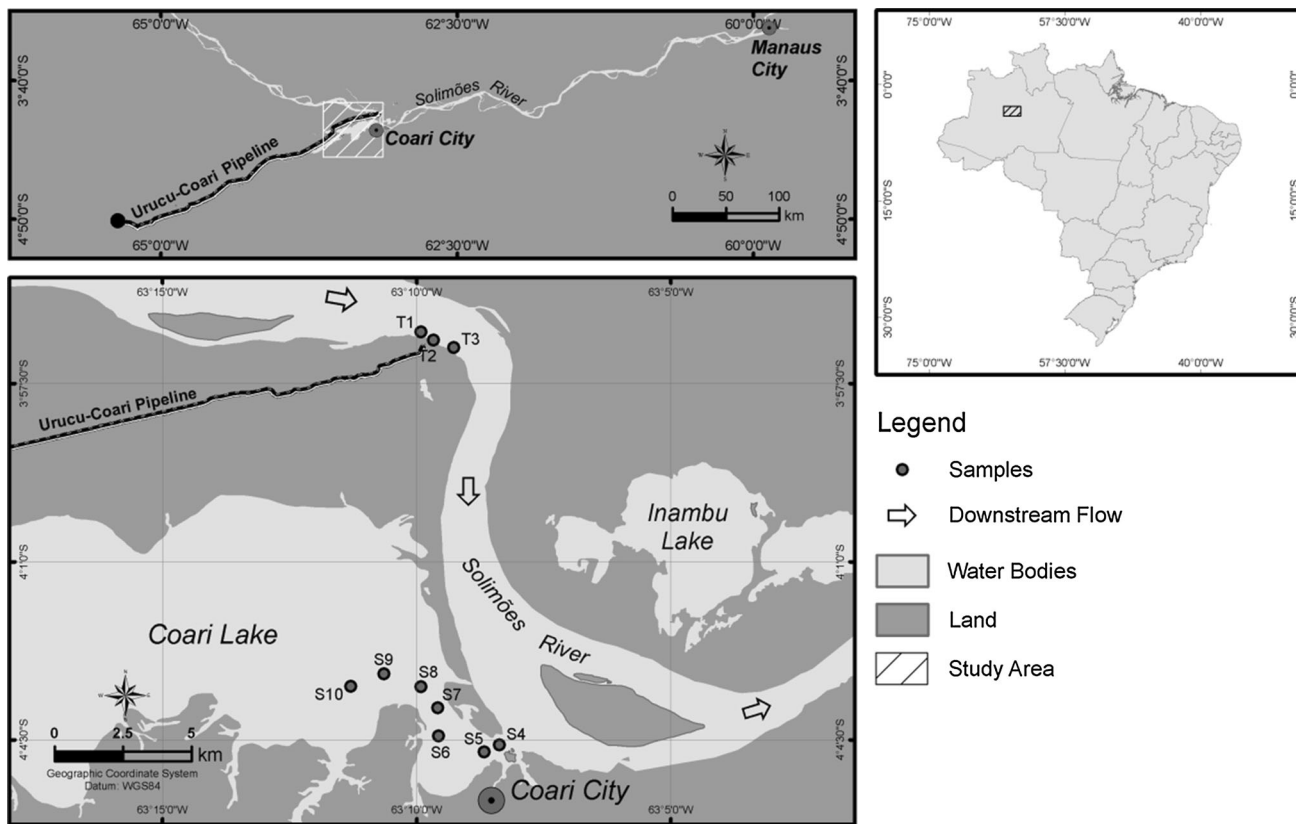
Fig. 1 Map showing the sediment samples collection locations in the Coari Lake and Solimões River

into the device, each sample was separated into two fractions: one larger and one smaller than 500 μm, due to the analytical capacity of the device (particles smaller than 500 μm). The organic carbon (C_{org}) was determined (wt/wt) using an Elemental Analyzer EA 1110 CHNS, CE instruments (Thermoquest, Italy).

Chemical standards

Perdeuterated standards (*n*-tetracosane-d_{50} and pyrene-d_{10}, 98 %, Cambridge Isotope Laboratories, Andovar, USA) were used as an internal standard and surrogate standards. A reference mixture of 16 PAHs (Absolute Standards, INC., USA), containing anthracene (An), benzo[a]anthracene (BaA), benzo[a]pyrene (BaP), benzo[b]fluoranthene (BbF), benzo[k]fluoranthene (BkF), benzo[g,h,i]perylene (BghiP), chrysene (Chry), dibenzo[a,h]anthracene (DBA), fluoranthene (Fl), fluorene (Fluo), indeno[1,2,3-cd]pyrene (InP), phenanthrene (Phe), perylene (Per) and pyrene (Py), was used as an external standard. The PAH mixture was further diluted with dichloromethane to prepare calibration solutions for gas chromatograph coupled to mass spectrometry (GC/MS) analyses. Standard solutions were stored at −20 °C. All solvents used to prepare and analyze the samples (dichloromethane, methanol and hexane) were of

chromatographic grade from Tedia Brazil (Rio de Janeiro, Brazil).

Extraction and isolation

The extraction was performed on approximately 30 g of dry sediment samples and 50 mL of dichloromethane/methanol solution (9:1) in an ultrasonic bath (Ultra Cleaner 800, UNIQUE) for 20 min at room temperature. This procedure was repeated three more times. The extracts were concentrated by rotary evaporation under reduced pressure and fractionated in a silica gel column. A suspension of 2.5 g of silica (previously activated for 24 h at 120 °C) in 10 mL *n*-hexane was added to the glass column (16 cm × 1.4 cm). The saturated hydrocarbon fraction was eluted with 10 mL of *n*-hexane, and the aromatic hydrocarbon fraction was eluted with 10 mL of *n*-hexane:dichloromethane (8:2). The fractions were concentrated by rotary evaporation under reduced pressure. The PAH fractions were completed to 100 μL with pyrene-d_{10} standard solution at 1 ng μL^{-1} and the aliphatic hydrocarbon fraction (AH) with 100 μL with *n*-tetracosane-d_{50} standard solution at 20 ng μL^{-1}. The analyses were carried out using gas chromatograph with flame ionization detector (GC-FID) and GC/MS for all organic compounds.

Gas chromatography–flame ionization detection (GC-FID) and gas chromatography–mass spectrometry (GC/MS)

The fractions obtained from the column chromatography were analyzed by GC-FID model 7890A and by GC/MS model 6890 and 5973, both from Agilent Technologies. Quantification and the profile of compounds were performed from GC-FID, and identification was evaluated with GC/MS. The analyses were performed with a HP-5MS fused silica capillary column with a stationary phase from Agilent Technologies, USA (J & W, 30 m × 0.25 mm i.d., 0.25 μm film thickness). The analytical conditions used were temperature increasing from 40 to 150 °C at 15 °C min^{-1} and from 150 to 310 °C at 3.0 °C min^{-1}, then maintaining a constant temperature for 10 min. The injector temperature was 300 °C, and the detector temperature was 320 °C. The carrier gas used in GC-FID was hydrogen (White Martins) and in GC/MS helium (White Martins); carrier gas flow was 1.5 and 1.0 mL min^{-1}, respectively. Splitless injection of 1 μL of sample was performed.

Data acquisition in GC/MS was in electron impact (70 eV), and selected ion monitoring (SIM) mode was used to identify and quantify PAH compounds (m/z 76, 101, 102, 106, 114, 126, 128, 138, 139, 152, 153, 165, 166, 178,179, 202, 212, 219, 228, 234, 252, 276 and 278). The standard PAH mixture was also analyzed in SIM mode in the mass range of 50–400 Da. Two characteristic ions were selected for each parent PAH for identifying SIM mode analyses via their retention times. In the aliphatic hydrocarbon fractions, the characteristic ions were analyzed in SIM mode as follows: m/z 191 for terpanes (hopanes) and m/z 217 for steranes. Furthermore, samples were analyzed in SIM mode to obtain the mass spectra. The identification of the compounds was performed by examination and comparison with literature mass spectra, interpretation, retention time and elution order.

Stable carbon isotopic ratios of n-alkanes (δ^{13}C)

The saturated hydrocarbon fraction (n-alkanes) was isolated using silica gel column as purification step for δ^{13}C analyses. A column of powdered copper was used to remove elemental sulfur from the apolar fractions, before submitting them to argentatious/silica thin layer chromatography using hexane as eluent. Substances with C–C double bonds form complexes with silver ions. Hence, olefinic substances can be separated from saturated hydrocarbons on thin layers of silica gel previously impregnated with silver nitrate. The thin layers can be prepared quickly, readily identified and isolated quantitatively (Santos et al. 2004).

The δ^{13}C analyses of n-alkanes were performed by a GC/C/IRMS system consisting of a Trace chromatograph connected to a Finnigan MAT spectrometer (Thermo Finnigan MAT) via a combustion interface (GC—Combustion interface III). The GC conditions were: DB-5 column, splitless injection, initial temperature of 40 °C with a rate of 12 °C min^{-1} until 120 °C, a rate of 3 °C min^{-1} until 300 °C and held at 300 °C for 15 min. For isotopic standardization, CO_2 (White Martins 99.995 %) reference gas was automatically introduced into the mass spectrometer in a series of three pulses at the beginning and the end of each analysis. Prior to carbon isotope analyses, the δ^{13}C of CO_2 reference gas was calibrated relative to the δ^{13}C of Vienna Pee Dee Belemnite (VPDB). The isotope data were tested using a mixture of n-alkanes with known δ^{13}C values acquired from Indiana University, USA (C_{16}–C_{30}). The intensity of the reference gas used in the analysis detection was 2000 mV. Thus, the intensity range assumed for the n-alkanes peaks has a slight deviation in the δ^{13}C which was between 300 and 1700 mV. Backgrounds lower than 100 mV were accepted for n-alkane analysis. The internal standard (n-tetracosane-d_{50}) was used as a control of the matrix influence on the δ^{13}C values of n-alkanes.

Quality control and quality assurance

The analytical method for the sediments was evaluated to provide credibility to the results and later applied to the samples. Sediment blank samples, pre-extracted several times and tested with chromatography methods demonstrating that there was no target analyte, were spiked with the standard solution of n-tetracosane-d_{50} and PAHs (16 PAHs plus perylene) at five different concentration levels. The results from blank samples were used to establish method detection limits (MDL). The MDL of each analyte was calculated as the average plus three standard deviations of its blank levels. For the compounds not detected in blank samples, MDLs were based on their instrumental detection limit. Thus, statistical evaluation of the method is given in Table 1.

Before analysis, standard solutions of n-tetracosane-d_{50} for GC-FID and of PAHs for GC/MS were run to check column performance, peak height and resolution. Each set of samples was run in sequence with a solvent blank; standard and a spiked sample were used to check method accuracy.

The limits of detection (LODs) (ICH 1995; INMETRO 2003) were calculated by using a signal-to-noise ratio of 3 (the ratio between the peak intensity under SIM condition and the intensity of the noise was used) and using recovery experiments at the lowest fortification level. The limits of quantification (LOQ) (ICH 1995; INMETRO 2003) were

Table 1 Results of analytical procedure of n-alkanes and PAHs

Compounds	Concentrations range (ng g^{-1})	Recovery (%)	RDS (%)	LOD (ng g^{-1})	LOQ (ng g^{-1})
n-alkane					
C$_{24}$d$_{50}$	25–500	63–85	7–24	1.6	5.7
PAHs					
BaA	5–80	70–97	5–23	0.01	0.05
BaP	5–80	67–102	6–14	0.13	0.30
BbF	10–80	76–93	19–28	0.06	0.30
BbghiP	5–80	70–90	2–28	0.01	0.06
BkF	10–80	65–96	11–33	0.05	0.21
Chry	20–80	85–101	6–14	0.05	0.20
DBA	5–80	64–92	5–21	0.01	0.10
Fluo	5–80	71–88	6–15	0.01	0.02
InP	5–80	74–89	4–12	0.14	0.50
Per	20–500	66–102	2–14	0.06	0.3
Phen	5–20	62–83	10–23	0.02	0.06
Py	5–80	63–94	5–26	0.01	0.03

RSD Relative standard deviation, *LOD* Limit of detection, *LOQ* Limit of quantification

calculated by using a signal-to-noise ratio of 10, always using the lowest fortification level.

The analytical curves obtained for the fortified sediments with the standard of n-tetracosane d-$_{50}$ and pyrene-d_{10} showed good linearity. Results demonstrated good accuracy (recovery between 62 and 102 %) and precision (below 33 %) of the analytical method. This analytical method was evaluated, and the quantification limit was in the range of 0.02–0.50 ng g^{-1} for PAHs and 0.1–5.7 ng g^{-1} for n-alkanes (Table 1).

Statistical analysis

Cluster analysis was performed with Statistica$^{®}$ 12.0 program from Statsoft (2013). For cluster analysis, we used the normalized data and Ward's method based on Euclidean distance. All data were assessed for normality and transformed as appropriate for this analysis. Significant factors were selected based on the Kaiser principle of accepting factors with eigenvalues >1. Factor loadings were considered significant if they were >0.7.

Results and discussion

Grain size analysis and organic carbon (C$_{org}$)

The grain sizes of the sediment samples were divided into three fractions: sand, silt and clay. The percent of sand varied from 0.7 to 26.5 %, silt varied from 71.3 to 86.4 %, and clay varied from 3.0 to 13.3 %. The distribution of individual particle size classes in the studied samples is

Table 2 Total percentage of the sand, silt and clay fractions in the samples

Samples	% Sand	% Silt	% Clay
T1	0.7	86.0	13.3
T2	10.0	81.7	8.3
T3	5.6	86.4	8.0
S4	18.4	74.2	7.4
S5	21.6	72.1	6.3
S6	13.5	83.5	3.0
S7	14.4	80.1	5.5
S8	26.5	68.1	5.4
S9	15.7	71.3	13.0
S10	12.5	80.3	7.2

given in Table 2. The predominant fraction is silt and small contributions from sand and clay. Sand may be due to soil leaching due to the increased hydrodynamics in the flooding period and to anthropogenic interference in the region. Surface samples from Coari Lake have shown the predominance of fine materials. The C$_{org}$ contents ranged from 0.29 to 1.99 %. Soil carbon present on the surface is associated with the labile fractions, while soil carbon is retained in the heavy fine fractions (clay and silt fractions). The deposits can be classified as mainly silty (Folk 1968). The samples are poorly to very poorly sorted. The fine-grained samples are generally better sorted than the coarse-grained ones.

The suspended load dominates in the sediment transport (Owens et al. 2005) although the bed load is significant at times. The relative low presence of clay-sized material

reveals that silt in all probability represents the prevalent active inorganic part of the sediment for pollutants. The studied modern fluvial deposits are generally fine grained. The increased content of the fine-grained sediment in modern rivers is generally assumed to be connected with human activity (Walling et al. 2000). Numerous contaminants and nutrients are transported and stored in association with the silt fraction (Horowitz et al. 1993; Foster and Charlesworth 1996; Owens et al. 2005).

Aliphatic hydrocarbons

In all samples, a homologous series of n-alkanes was found primarily between C_{17} and C_{35}, with C_{max} at C_{29} or C_{31} (additional data are given in Online Resource 1), which is indicative of the contribution of waxes from vascular plants in the sediment (Silva et al. 2013; Salem et al. 2014; Bícego et al. 1996). The predominance of n-alkanes with odd number carbons was observed, and it is an indication of contributions from terrestrial sources (Wang et al. 2013) (Table 3). The concentrations of total aliphatic hydrocarbons in the samples varied from 98.6 to 3470.7 ng g^{-1} of dry sediment (Table 3). These values are far below those of other studies performed in lakes and rivers from more urbanized sites, such as the central area of Campo dos Goytacazes (1200–4300 ng g^{-1}) (Gomes and Azevedo 2003) and in the Mundaú–Manguaba estuarine–lagoon system in Maceió (27,800–139,500 ng g^{-1}) (Silva et al. 2013). However, our values were higher than those found in the Red Sea sediments, Egypt (33.97–553.48 ng g^{-1}) (Salem et al. 2014) and similar to values of Antarctica (27.0–2890 ng g^{-1}) (Bícego et al. 1996) and marine sediments and soils at Davis Station, Antarctica (79.0–2240 ng g^{-1}) (Green and Nichols 1995).

The C_{19} and C_{20} isoprenoids, pristane (Pr) and phytane (Ph), respectively, are assumed to be end products from the phytyl side chain of chlorophyll a in the aquatic environment and may represent the input of algae, diatoms and phytoplankton (Wang et al. 1999). Whether Pr or Ph is formed from degradation of phytol depends on the toxicity of the environment (Didyk et al. 1978; Rontani et al. 1990; Elias et al. 2000). The studied samples have Pr/Ph in the range 0.05–1.09, indicating that the organic matter was subjected to an anoxic, highly reductive conditions (Peters et al. 2005; Texeira et al. 2014). Elias et al. (2000) also reported in their study in the Amazon that Pri/Phy ratio values close to 1 were found in samples close to the source of rivers and could be the result of a mixture of allochthonous and autochthonous contributions.

CPI values analyses revealed that they ranged between 2.4 and 5.0. It showed values above 1 but below 4 which generally suggest a mixture of oil plus biogenic sources like higher plants (Bakhtiari et al. 2010). One possible cause can be the multiple sources of n-alkanes in the study area. Meanwhile, the CPI values close to one are also thought to indicate greater inputs from marine microorganisms and/or recycled organic matter (Kennicutt et al. 1987). These findings seem to be consistent with the data previously reported by some researchers (Pearson and Eglinton 2000; Reddy et al. 2000).

Hopanes were detected in all samples (Table 4); the m/z 191 ion chromatogram of the studied samples showed a hopane series with molecules varying from C_{27} to C_{33}. Samples from the Solimões River (T1, T2 and T3) showed high levels of M29, Tβ, Hop-17(21)-ene and des-A-lupane (Fig. 2a). Tβ, M_{29}, H31R and H31ββ are the members with the highest concentrations in the Coari Lake sediments (Fig. 2b). Steranes and diasteranes were not detected.

In this study, there is no UCM (unresolved complex mixture) in all sediment samples (Fig. 2c). UCM is generally evidenced by a characteristic increase in the baseline of the chromatograms. A previous study suggested that a level of UCM lower than 10 µg g^{-1} in sediments indicated no petroleum contamination (Elias et al. 2000; Tolosa et al. 1996, 2004).

In the majority of sites, the peak relative to the compound Ts was larger than the Tm peak, indicating the sediment maturity because Ts is formed from Tm (Fig. 2) (Philp 1985). A contribution of hopanoids of biogenic origin, such as diploptene, hop-17(21)-ene and 17β(H),21β(H)-homohopane, was detected. This feature indicates bacterial contribution to the organic matter (Peters et al. 2005). Hopanes with a ββ configuration, such as 17β(H),21β(H)-homohopane, are not found in petroleum because it is thermally unstable during early catagenesis (Peters et al. 2005). On the other hand, hopanes with the 17α, 21β(H) configuration (αβ) in the range C_{27}–C_{35} are characteristic of petroleum due to their greater thermodynamic stability compared with the other epimeric series (ββ and βα). The major precursors for the hopanes in source rocks and crude oils include bacteriohopanetetrol and related bacteriohopanes, which show that the biological configuration is nearly flat, although puckering of the carbon–carbon bonds in the rings results in a three-dimensional shape. Bacteriohopanetetrol is amphipathic because it contains both polar and nonpolar ends. The flat configuration and amphipathic character are necessary for bacteriohopanetetrol to fit into the lipid structure (Peters et al. 2005; Rohmer 1987). Because this stereochemical arrangement is thermodynamically unstable, diagenesis and catagenes are of bacteriohopanetetrol result in the transformation of the 17β, 21β(H)-precursors to the 17α, 21β(H)-hopanes and 17β, 21α(H)-moretanes (Peters et al. 2005).

From C_{31} and C_{33}, the hopanes occur in pairs of stereoisomers and can have a 22R or 22S configuration.

Table 3 Compounds identified and quantified (ng g^{-1}) in the aliphatic fractions

Compounds	Characteristic ions (m/z)	T1	T2	T3	S4	S5	S6	S7	S8	S9	S10
n-Hexadecane	85/226	<Q.L.	<Q.L.	<Q.L.	<Q.L.	<Q.L.	<Q.L.	4.1	4.0	18.7	21.2
n-Heptadecane	85/240	7.1	4.5	0.7	4.0	9.6	9.7	13.7	18.2	136.7	42.5
Pristane	183/268	7.1	4.5	0.7	4.0	9.6	9.7	13.7	18.2	136.7	42.5
3-Methyl-heptadecane	85/254	2.2	2.0	0.1	1.0	1.8	1.1	5.4	4.6	24.0	13.2
n-Octadecane	85/254	1.8	1.6	0.1	<Q.L.	1.5	2.3	2.2	3.2	5.4	4.4
Phytane	183/282	17.2	10.3	5.5	2.0	8.2	9.7	9.7	15.4	34.2	27.0
n-Nonadecane	85/268	7.3	3.7	2.0	0.9	3.9	2.6	3.8	6.1	57.2	14.0
9-Octil-heptadecane	85/352	20.3	10.8	9.5	2.0	11.4	11.7	11.3	25.9	89.4	66.9
n-Eicosane	85/282	1.2	0.5	0.6	<Q.L.	11.9	4.3	6.1	1.8	32.3	3.3
n-Heneicosane	85/296	26.4	16.1	12.9	1.8	14.3	20.3	15.3	29.6	47.4	44.2
n-Docosane	85/310	26.5	18.7	17.9	2.3	19.9	25.0	21.0	47.1	82.5	59.9
n-Tricosane	85/324	26.7	16.9	14.5	1.5	18.8	21.7	19.4	26.2	45.0	41.1
n-Tetracosane	85/338	42.5	36.0	28.5	3.3	34.4	33.8	39.0	55.0	129.8	1116
n-Pentacosane	85/352	101.1	218.5	219.1	2.3	80.2	47.5	61.6	131.2	147.0	156.9
n-Hexacosane	85/366	1.7	61.7	50.8	4.7	51.7	49.7	62.9	85.8	195.6	204.2
n-Heptacosane	85/380	36.7	24.9	20.8	2.5	27.5	36.4	29.0	43.2	94.7	91.8
n-Octacosane	85/394	129.9	130.8	99.6	7.2	80.1	72.7	91.7	138.1	294.9	290.8
n-Nonacosane	85/408	59.0	45.4	39.1	3.4	38.0	45.0	38.2	61.5	118.2	116.1
n-Triacontane	85/422	408.1	555.0	476.0	21.7	233.8	122.3	196.1	368.2	563.7	492.6
n-Hentriacontane	85/436	76.3	70.4	59.6	3.7	42.5	47.3	45.7	79.5	136.7	147.3
n-Dotriacontane	85/450	432.4	498.0	431.3	17.2	225.8	149.9	205.3	379.2	633.8	590.5
n-Tritriacontane	85/464	62.1	59.9	49.7	2.1	2.7	38.3	31.7	58.3	104.1	113.2
n-Tetratriacontane	85/478	158.0	156.9	140.8	3.8	80.7	68.9	72.1	145.8	272.2	260.8
n-Pentatriacontane	85/492	14.9	9.4	6.8	<Q.L.	5.9	8.9	7.6	11.3	18.5	18.2
Des-A-Lupane	123/330	100.5	212.5	215.1	11.1	79.4	48.0	59.8	124.7	143.4	151.4
Total aliphatic hydrocarbons		1791.7	2176.2	1917.8	98.6	1096.8	886.5	1059.6	1892.4	3470.7	3131.2
Total n-alkanes		1678.6	1955.8	1699.9	85.0	998.4	828.2	982.3	1752.0	3208.2	2945.0
CPI		3.9	5.0	4.9	4.3	4.6	2.4	3.6	3.7	3.7	3.4
Pr/Ph		0.30	0.54	0.05	1.09	0.46	0.42	0.21	0.75	0.42	0.94
C$_{max}$		C31	C29	C29	C29	C29	C31	C31	C31	C31	C31

CPI carbon preference index CPI $= 1/2$ $[(\sum_{odd}C_{25}-C_{33})/(\sum_{even}C_{24}-C_{32}) + (\sum_{odd}C_{25}-C_{33})/(\sum_{even}C_{26}-C_{34})]$; *C$_{max}$* major component, *Pr* pristane and *Ph* phytane, *<Q.L.* lower than quantification limit

According to Peters et al. (2005), S compounds contribute more than R compounds to the composition of oil. The H31R epimer appears to have predominance over H31S in all sites along Coari Lake, indicating there are no hydrocarbons from petroleum and derivatives in the site. In the Solimões River, site T1 showed similar values for H31R and H31S, and sites T2 and T3 showed a greater H31S epimer concentration (Fig. 2a). Therefore, there is the possibility of some type of petroleum contamination near the TESOL. The relationship between the H32 (R and S) and H33 (R and S) epimers varied a great deal among samples, making it difficult to identify and confirm petroleum contamination. The S7, S9, S10 and T1 samples showed higher H32R epimer concentrations, while the samples S4, S5, S8, T2 and T3 showed a higher homolog H32S concentration. Site S6 had equivalent amounts of the isomers. Interestingly, site T1, upstream from the TESOL, did not show contamination, and only sites downstream from the terminal showed contamination signs. Additionally, in Coari Lake, the sites that showed higher contamination signs were located closer to the lake entrance, which may be due to the contribution of material from the Solimões River or from ships anchored at Coari.

The triterpenoid des-A-lupane was detected in all samples. The identified triterpenoids and des-A-triterpenoids of the structural classes of oleanane, lupane, ursane and

Table 4 Hopanes identified in the samples

Abbreviation	Hopane	Molecular formula	T1	T2	T3	S4	S5	S6	S7	S8	S9	S10
Ts	18α(H)- 22,29,30-trisnorneohopane	$C_{27}H_{46}$	+	+	+	+	+	+	+	+	+	+
Tm	17α(H)- 22,29,30-trisnorhopane	$C_{27}H_{46}$	+	+	+	+	+	+	+	+	+	+
Tβ	17β(H)- 22,29,30-trisnorhopane	$C_{27}H_{46}$	+	+	+	+	+	+	+	+	+	+
H29	17α(H), 21β(H)-30-norhopane	$C_{29}H_{50}$	+	+	+	+	+	+	+	+	+	+
29Ts	18α(H), 21β(H)-30-norneohopane	$C_{29}H_{50}$	+	+	+	+	+	+	+	+	+	+
H$\Delta_{22(29)}$	17β(H)-hop-22(29)-ene (diploptene)	$C_{30}H_{50}$	+	+	nd	nd	nd	+	nd	+	+	+
M29	17β(H), 21α(H)-30-norhopane (normoretane)	$C_{29}H_{50}$	+	+	+	+	+	+	+	+	+	+
H30	17α(H), 21β(H)-hopane	$C_{30}H_{52}$	+	+	+	+	+	nd	+	+	+	+
H31S	17α(H), 21β(H),22S-homohopane	$C_{30}H_{52}$	+	+	+	+	+	+	+	+	+	+
H31R	17α(H), 21β(H),22R-homohopane	$C_{30}H_{52}$	+	nd	+	+	+	+	+	+	+	+
H$\Delta_{17(21)}$	Hop-17(21)-ene	$C_{30}H_{50}$	+	+	+	+	+	+	+	+	+	+
H32S	17α(H), 21β(H),22S-bishomohopane	$C_{32}H_{56}$	+	+	+	+	+	+	+	+	+	nd
H32R	17α(H), 21β(H),22R-bishomohopane	$C_{32}H_{56}$	+	+	+	+	+	+	+	+	+	+
H31ββ	17β(H), 21β(H)-homohopane	$C_{31}H_{54}$	+	+	+	+	+	+	+	+	+	+
H33S	17α(H), 21β(H),22S-trishomohopane	$C_{33}H_{58}$	nd	+	+	nd	+	+	+	+	+	+
H33R	17α(H), 21β(H),22R-trishomohopane	$C_{33}H_{58}$	nd	nd	nd	nd	nd	+	nd	nd	nd	nd

nd = not detected, $+$ = detected but not quantified

friedelane are characteristic of angiosperms (Otto et al. 2005). The presence of des-A-lupane in the sediments also suggests that microbial and photochemical processes contributed to the organic matter alteration (Otto et al. 2005).

Stable carbon isotopic composition (δ¹³C)

The nature of the Coari sedimentary organic matter was examined using compound-specific $\delta^{13}C$ analysis of individual n-alkanes. The stable carbon isotopic ratios of n-alkanes ($\delta^{13}C$) compositions of all detected n-alkanes in the sediment samples fall in the range between -35.0 and -23.1 ‰ (Table 5), suggesting an isotopic composition reflecting mainly C_3 plants and algae (Pancost and Boot 2004). The typical $\delta^{13}C$ values of terrestrial plants with C_3 pathway range from -33 to -22 ‰, average at -27 ‰ (Pancost and Boot 2004).

A "zigzag" pattern is apparent (Fig. 3) mainly in the short-chain members ($C_{16}–C_{25}$), while for $C_{26}–C_{33}$, no significant variation was observed. This difference in isotope composition of odd-to-even n-alkanes reveals different origins and occurs only for low lake level. It is characterized by an extension of organic detritus accumulation, sometimes even organic anthropogenic layers (Silva et al. 2008; Magny 2004; Galka and Apolinarska 2014). The odd-numbered n-alkanes found in sediments may come from vegetation by decarboxylation of even-numbered fatty acids of waxes from higher plants (Silva et al. 2008; Maioli et al. 2012; Ishiwatari et al. 1994). On the other hand, petroleum derivatives are more depleted in $\delta^{13}C$ in comparison with recent biomass. The "zigzag"

pattern could be used to infer mixture of biogenic and anthropogenic sources (Maioli et al. 2012). The $\delta^{13}C$ values for $C_{26}–C_{33}$ n-alkanes of recent sediments from Coari Lake showed that there are no isotopic differences between odd- and even-numbered n-alkanes. The biogenic sources show $\delta^{13}C$ values for the n-alkanes with no "zigzag" pattern ($C_{26}–C_{33}$). In contrast, a mixture of biogenic and anthropogenic sources shows this pattern ($C_{16}–C_{25}$).

Aromatic hydrocarbons

In the ten analyzed samples, 31 aromatic compounds were identified (additional data are given in Online Resource 1). The total concentration of aromatic hydrocarbons in the samples varied from 46.33 to 1253.66 ng g^{-1} of dry sediment (Table 6).

The chromatographic profiles of the sediments collected at Coari Lake were similar at all the sites, although the profiles differed from those found in the samples analyzed from the Solimões River (Fig. 4).

The sites sampled in the Solimões River (T1, T2 and T3) showed a large perylene concentration, varying from 173.34 to 219.70 ng g^{-1} of sediment; however, the sites from Coari Lake did not exhibit the same perylene concentrations that varied between 0.82 and 10.31 ng g^{-1} of sediment, and perylene was not detected at site S6 (Table 6). Perylene is an indicator of diagenetic conditions, and its genesis may be process-governed and independent of the type of organic matter within the sediment. Moreover, perylene may form from non-specific precursor materials by microbial processes (Silliman et al. 1998).

Fig. 2 a Partial *m/z* 191 mass chromatogram from the Solimões River (T2), **b** partial *m/z* 191 mass chromatogram from the Coari Lake (S7) and **c** GC-FID chromatograms of aliphatic hydrocarbons from the Solimões River (T2). *Hopanes Ts* 18α(H)-22,29,30-trisnorneohopane; *Tm* 17α(H)-22,29,30-trisnorhopane; *Tβ* 17β(H)-22,29,30-trisnorhopane; *H29* 17α(H),21β(H)-30-norhopane; *29Ts* 18α(H),21β(H)-30-norneohopane; *HΔ₂₂₍₂₉₎* 17β(H)-hop-22(29)-ene; *M29* 17β(H),21α(H)-30-norhopane; *H30* 17α(H),21β(H)-hopane; *H31S* 17α(H),21β(H),22S-homohopane; *H31R* 17α(H),21β(H),22R-homohopane; *HΔ₁₇₍₂₁₎* Hop-17(21)-ene; *H32S* 17α(H),21β(H),22S-bishomohopane; *H32R* 17α(H),21β(H),22R-bishomohopane; *H31ββ* 17β(H), 21β(H)-homohopane; *H33S* 17α(H),21β(H),22S-trishomohopane; H33R: 17α(H),21β(H),22R-trishomohopane
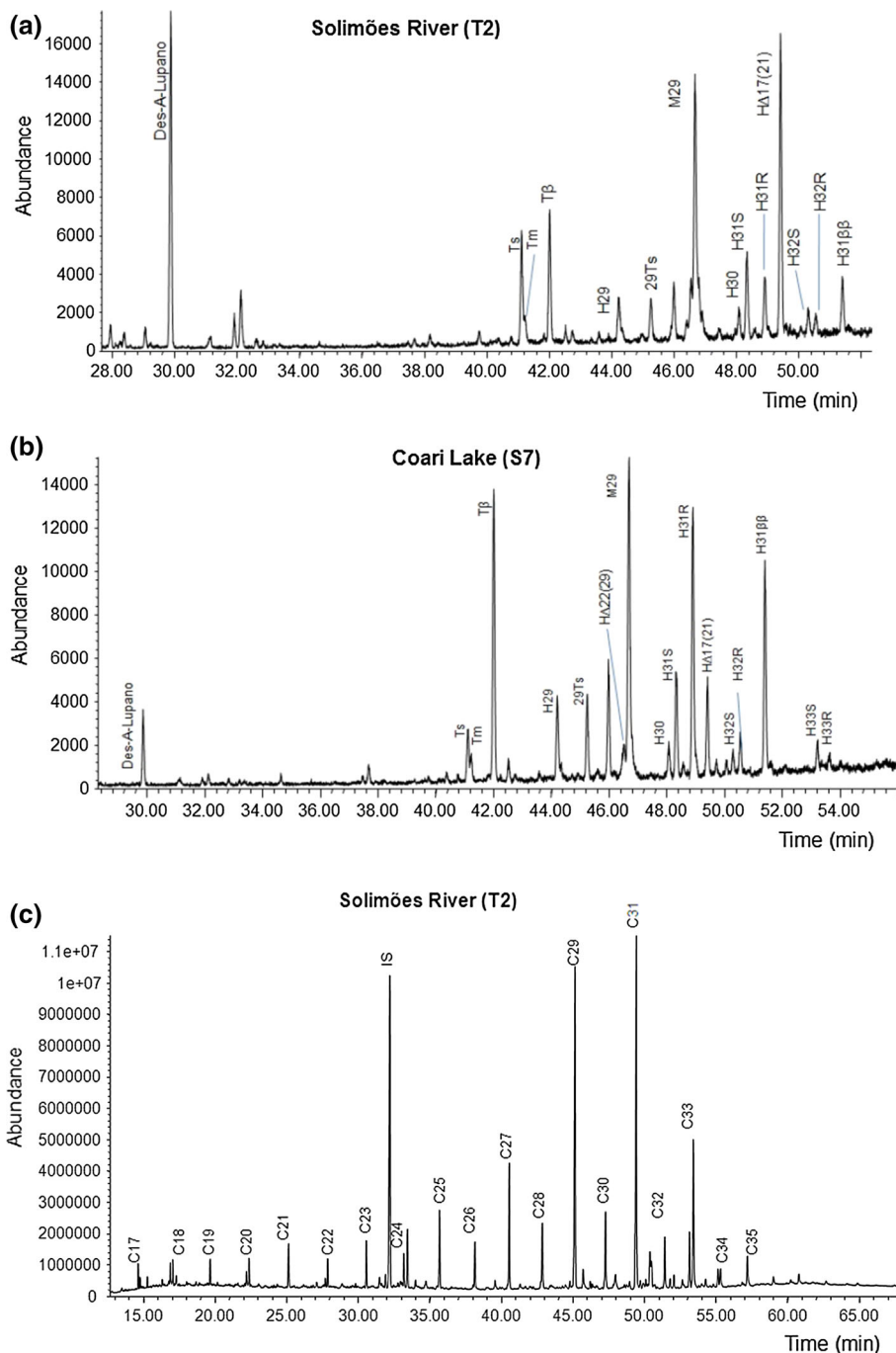

PAHs of biogenic origin, such as retene, cadalene and (ring A) monoaromatic lupane, were also identified. Retene (1-methyl-7-isopropyl-phenanthrene) derives from abietic acid, a natural diterpenoid constituent of plant resin. In addition to its natural occurrence, retene can also be a wood combustion marker (Simoneit 1977). Retene was not found in large quantities compared to the perylene concentration in the studied samples, having a maximum concentration of 8.84 ng g⁻¹ at site S8 and not being detected at sites T2, T3 and S6 (Table 6). Cadalene is the

final product of the diagenetic degradation of compounds of cadinene-type compounds and, as a consequence, is the most common sesquiterpene reported in sediments (Elias et al. 1996). The cadalene concentration varied from 0.19 to 8.79 ng g⁻¹, with the exception of the sampling sites S6, S7 and S8, where cadalene was not detected. Ring A monoaromatic lupane is a pentacyclic triterpenoid derived from lupeol and is formed through the diagenesis of plant precursors and natural products (Gomes and Azevedo 2003). The highest concentrations of monoaromatic lupane

Table 5 $\delta^{13}C$ values of individual n-alkanes from C_{16} to C_{33} for an Amazon lake system, Brazil

	C_{16}	C_{17}	C_{18}	C_{19}	C_{20}	C_{21}	C_{22}	C_{23}	C_{24}
T1	−24.56	−30.75	−28.13	−28.33	−28.67	−30.56	−32.16	−33.51	−23.23
T2	−24.44	−31.72	−27.33	−28.76	−28.16	−32.58	−26.31	−31.98	−24.83
T3	−24.58	−31.95	−28.24	−27.19	−28.11	−31.87	−28.96	−29.99	−24.56
S4	−25.36	−29.98	−28.30	−28.69	−27.95	−30.24	−29.34	−34.58	−26.21
S5	−24.74	−30.57	−27.05	−27.51	−26.87	−30.54	−30.01	−34.01	−25.39
S6	−25.42	−30.67	−27.74	−29.47	−27.23	−31.68	−29.47	−33.98	−24.28
S7	−25.68	−31.23	−27.65	−29.57	−29.32	−32.39	−28.91	−34.32	−23.45
S8	−24.87	−31.24	−28.32	−27.55	−27.67	−30.08	−27.63	−33.24	−25.87
S9	−24.39	−31.85	−28.16	−29.04	−29.03	−31.62	−32.15	−32.15	−26.53
S10	−25.19	−30.25	−28.31	−28.74	−28.54	−32.02	−28.64	−32.36	−23.06

	C_{25}	C_{26}	C_{27}	C_{28}	C_{29}	C_{30}	C_{31}	C_{32}	C_{33}
T1	−32.98	−32.65	−33.96	−32.70	−33.38	−33.82	−34.26	−34.70	−34.13
T2	−30.24	−30.76	−32.01	−31.57	−31.49	−31.48	−31.48	−32.13	−32.54
T3	−31.58	−30.95	−31.81	−32.65	−34.58	−31.98	−32.58	−32.48	−33.26
S4	−32.35	−32.15	−31.24	−32.47	−34.12	−32.38	−34.98	−33.54	−31.47
S5	−31.85	−30.78	−32.89	−32.32	−33.18	−33.54	−34.64	−34.98	−34.69
S6	−32.34	−32.74	−32.56	−32.83	−34.98	−34.18	−33.47	−32.74	−34.23
S7	−30.26	−32.32	−33.54	−31.74	−33.56	−33.85	−31.69	−32.08	−34.87
S8	−32.56	−30.14	−31.49	−31.56	−34.58	−32.12	−34.87	−34.86	−33.74
S9	−31.95	−31.55	−32.78	−30.79	−33.92	−34.74	−32.62	−34.01	−33.52
S10	−32.71	−31.72	−30.98	−30.95	−31.14	−33.14	−34.93	−31.25	−32.04

Fig. 3 Profiles of n-alkane isotopic composition (from C_{16} to C_{33}) in surface sediments from Coari Lake, Amazon region, Brazil
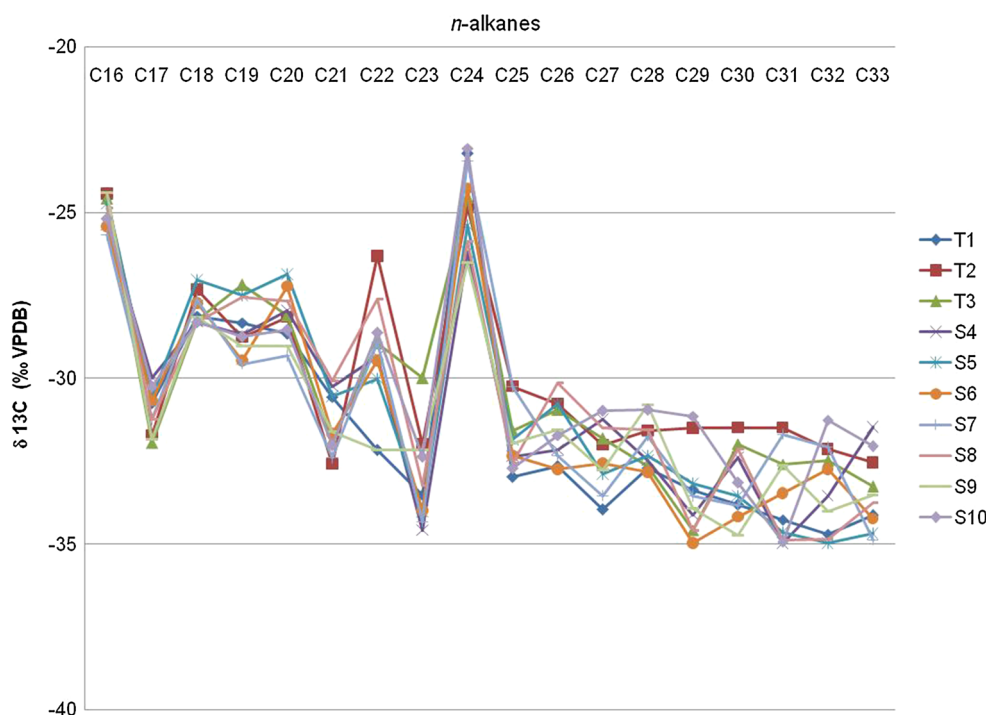
were found at T2 and T3, in agreement with the results for perylene, which also exhibited the highest values in the samples from the Solimões River.

In addition to these biogenic origin aromatic hydrocarbons, various biogenic origin aromatic hydrocarbons derived specifically from α and β-amyrin were found; these

Table 6 Aromatic hydrocarbons identified and quantified (ng g^{-1})

No	Compounds	RT (min)	m/z	T1	T2	T3	S4	S5	S6	S7	S8	S9	S10
1	Dimethyl(methyl-ethyl) Naphthalene (Cadalene)	12.2	183/198	0.38	0.19	0.36	1.44	0.96	<Q.L.	<Q.L.	<Q.L.	8.79	1.82
2	Dihydro-trimethyl-phenyl-1H-Indene	12.9	221/236	0.13	0.11	<Q.L.	51.72	24.35	16.38	0.86	51.93	66.32	41.36
3	Phenanthrene	14.2	178/179	0.41	0.43	0.37	1.90	1.35	0.53	0.05	1.58	5.68	2.87
4	Anthracene	14.3	178/179	0.31	0.24	0.24	2.47	0.66	0.64	0.05	1.79	5.68	2.72
5	Methyl-phenanthrenes	16.8–17.5	192/191	9.42	1.81	2.47	10.13	6.69	2.17	0.12	11.01	16.27	9.43
6	Dimethyl-phenanthrenes	19.7–20.6	206/189	10.32	3.22	5.56	10.82	8.77	1.25	0.13	9.99	11.11	7.29
7	Fluoranthene	20.8	202/101	2.85	1.41	1.61	2.41	1.99	0.12	0.03	3.81	3.98	2.98
8	Pyrene	22.1	202/101	2.84	0.67	1.31	2.14	1.53	0.02	0.02	3.12	4.06	3.08
9	Trimethyl-phenanthrenes	23.0 – 23.6	220/205	6.12	1.97	2.92	6.06	4.23	<Q.L.	0.03	4.79	5.42	3.31
10	1-Methyl-7-isopropyl-phenanthrene (Retene)	24.8	219/234	0.64	<Q.L.	<Q.L.	0.90	0.91	<Q.L.	0.57	8.83	1.26	0.94
11	Benzo(g, h, i)fluoranthene	29.1	226	<Q.L.	<Q.L.	<Q.L.	<Q.L.	<Q.L.	<Q.L.	<Q.L.	1.75	<Q.L.	1.47
12	3,3,7,12a-Tetramethyl-octahydro chrysene	30.6	292/293	1.86	18.13	21.80	16.46	9.29	<Q.L.	2.14	6.45	13.64	11.08
13	Chrysene	30.8	228/114	2.71	1.90	2.38	4.65	<Q.L.	0.84	2.70	0.70	4.45	3.10
14	Des-A-tetramethyl chrysene diaromatic	31.1	207/292	0.75	14.02	20.48	20.31	6.41	<Q.L.	0.74	4.23	7.74	5.44
15	Des-A-lupa-diaromatic—tetracyclic triterpenoid derived from Lupeol	31.5	292/207	0.54	14.60	18.86	6.92	3.65	<Q.L.	0.72	5.15	5.81	7.33
16	Des-A-trimethyl chrysene triaromatic—triterpenoid tetracyclic derived from β-amyrin	33.7	231/274	4.05	7.25	7.39	9.06	5.56	1.42	4.19	4.24	7.44	5.69
17	Des-A-trimethyl chryseno triaromatic—tetracyclic triterpenoid derived from α-amyrin (3,4,7-trimethyl-1,2,3,4-tetrahydro chrysene)	34.7	259/274	4.25	14.40	13.95	6.47	6.23	1.77	3.84	2.71	7.28	3.96
18	3,3,7-trimethyl-1,2,3,4-tetrahydro chrysene	35.2	218/274	6.50	27.23	35.03	38.79	18.01	0.03	6.54	16.99	39.82	13.04
19	Benzo[b]fluoranthene	38.1	252/126	1.69	1.50	1.43	3.51	<Q.L.	1.27	2.14	1.38	5.91	4.06
20	Benzo[k]fluoranthene	39.7	252/126	1.28	1.62	1.65	2.65	<Q.L.	1.22	1.77	<Q.L.	1.94	1.77
21	Perylene	40.5	252/125	219.70	173.34	210.88	4.28	1.27	<Q.L.	0.82	9.44	10.31	3.88
22	Dinorolean monoaromatic—triterpenoid derived from α amyrin (Ursan-12-ene)	44.0	145/158	3.16	79.80	88.73	18.65	18.07	1.55	3.39	31.15	24.40	14.03
23	Olean-12-ene monoaromatic ring A	45.1	145/158	1.16	43.70	51.24	11.93	4.34	0.86	1.14	13.24	4.44	3.57
24	Dinorlupa monoaromatic—pentacyclic triterpenoid derived from lupeol (Lupane monoaromatic ring A)	45.4	145/378	8.90	156.20	160.70	49.19	29.07	2.39	9.17	58.99	26.60	16.42
25	Lupatriaromatic—pentacyclic triterpenoid derived from Lupeol	47.2	342/343	5.07	54.27	84.93	32.02	16.87	1.23	5.10	18.28	14.91	10.32
26	Tetramethyl piceno triaromatic—pentacyclic triterpenoid derived from β-amyrin	47.5	257/342	3.97	41.88	76.01	38.15	10.47	1.76	4.78	16.44	12.59	9.10

Table 6 continued

No	Compounds	RT (min)	m/z	T1	T2	T3	S4	S5	S6	S7	S8	S9	S10
27	Aromatization of Lupane	47.7	342/257	2.52	33.86	59.46	18.22	8.47	1.14	2.81	16.93	10.42	4.74
28	Aromatization of β-Amyrin	47.9	310/254	6.63	33.97	36.53	38.74	9.33	3.93	7.58	2.24	15.95	8.30
29	Trimethyl picene tetraaromatic—pentacyclic triterpenoid derived from α-amyrin	50.7	324/309	6.35	37.58	127.85	26.39	8.95	1.19	6.70	3.33	14.43	9.76
30	Trimethyl picene tetraaromatic—pentacyclic triterpenoid derived from β-amyrin	51.2	324/268	16.83	88.66	169.43	1.06	21.98	1.57	15.58	12.87	35.95	22.59
31	Lupa tetraaromatic—pentacyclic triterpenoid derived from Lupeol	52.4	324/309	3.25	65.22	50.09	18.50	3.75	<Q.L.	2.48	<Q.L.	4.97	3.15
	Total aromatic hydrocarbons			337.35	920.09	1253.66	456.73	235.32	46.33	88.97	327.44	458.83	242.86

<Q.L. lower than quantification limit., RT retention time

compounds are triterpenoids derived from higher plants (Rogge et al. 2007). These derivatives include triaromatic des-A-trimethylchrysene, monoaromatic dinoroleane, triaromatic tetramethylpicene, 3,3,7-trimethyl-1,2,3,4-tetrahydrochrysene, tetraaromatic trimethylpicene and monoaromatic ursan-12-ene (Table 6). The majority of the plant-derived aromatic compounds were present at higher concentrations in the Solimões River (T2 and T3), most likely due to the greater number of trees on the Solimões River banks.

Among the aromatic compounds found in the samples, seven are included on the priority pollutants list from the United States Environmental Protection Agency (US-EPA): anthracene, phenanthrene, fluoranthene, pyrene, chrysene, benzo[b]fluoranthene and benzo[k]fluoranthene.

The concentration of these PAHs in the samples varied from 4.64 to 31.70 ng g^{-1} of dry sediment. Sites S5 and S6 showed the lowest concentrations of these PAHs. The distribution profile of priority PAHs in the samples showed that the site with the highest concentration of PAHs was S9, followed by S10, which also showed a very homogeneous distribution of these PAHs.

The PAH concentrations found in the samples are well below those established by Canadian Interim Freshwater Sediment Quality Guidelines (ISQGs) (Canadian Council of Ministers of the Environment 2001), indicating an uncontaminated environment (Table 7). This value indicates the sediment quality capable of sustaining the environment's primary functions, protecting the ecological receptors and groundwater quality. Additionally, comparing the total PAH concentrations found in this study (4.64–31.70 ng g^{-1}) with other regions in Brazil and worldwide, such as Guanabara Bay (77 to 7751 ng g^{-1}) (Silva et al. 2007), Manguaba Lagoon (29.2–222.7 ng g^{-1}), Mundáu River (86.0–208.4 ng g^{-1}), Mundáu Lagoon (41.1–100.9 ng g^{-1}) (Silva et al. 2013) and the Nile River (53.4–5558.0 ng g^{-1}) (Havelcováa et al. 2014), the concentrations in the studied samples are much lower, indicating that the studied location is well preserved. These results are similar to an environmental protection area in the SW Atlantic, Laranjeiras Bay, Brazil (3.85–89.1 ng g^{-1}) (Martins et al. 2012), and a little higher than the compounds in the benthic environment of a subtropical embayment, Ubatuba Bay, Brazil (0.16–3.76 ng g^{-1}) (Muniz et al. 2006).

The An/178 ratio had values greater than 0.1 for all sites. This result indicates the contribution of pyrogenic sources in the sediments (Fig. 5a). Moreover, the Fl/(Fl + Py) ratio indicates that the combustion was derived from biomass burning for the majority of sites (Fig. 5b).

Hierarchical cluster analysis is an important tool that groups samples according to their similarities. Within the same group, samples have the greatest similarities, while between groups they have the lowest similarities (Moita

Fig. 4 Mass chromatograms
characteristic of aromatic
hydrocarbons from (a) the
Solimões River (T2) and
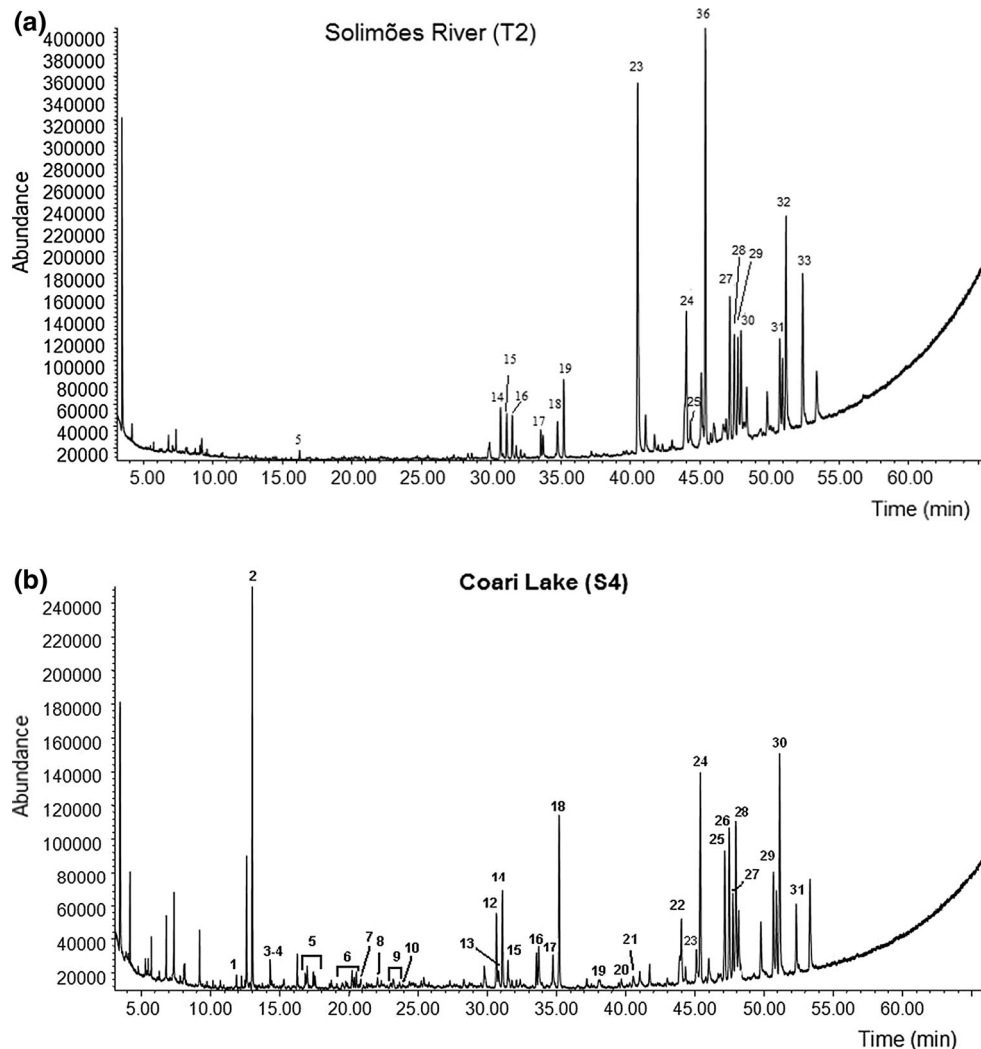(b) Coari Lake (S4). Numbers
on the peaks in Table 5

Table 7 Guiding values of
PAHs concentrations in
freshwater superficial sediment
(ISQGs, 2001)

Compounds	Sediment (ng g^{-1} dry weight) (ISQGs)	The present study (ng g^{-1})
Anthracene	46.9	0.05–2.72
Benzo(a)anthracene	31.7	<Q.L.
Chrysene	57.1	0.70–4.65
Dibenzo(a,h)anthracene	6.22	<Q.L.
Phenanthrene	41.9	0.05–11.36
Naphthalene	34.6	<Q.L.
Pyrene	53.0	0.02–4.06
Fluoranthene	111.0	0.03–3.98

ISQGs Interim freshwater sediment quality guidelines, *<Q.L.* lower than quantification limit

Neto and Moita 1998). Variables represent good correlation observed between the river analysis (T1, T2, T3), Coari Lake (S6, S7, S8, S9 and S10) and mixture of river plus lake (entrance of the river, S4). Three distinct groups were formed from the cluster analysis. The samples

correlation with a specific compound suggests that each group has a specific origin. The first group is compounds from Coari Lake with lower perylene concentration and higher contribution of pyrogenic origin. Second group, S4 site, is characterized by a mixture of sources (river and
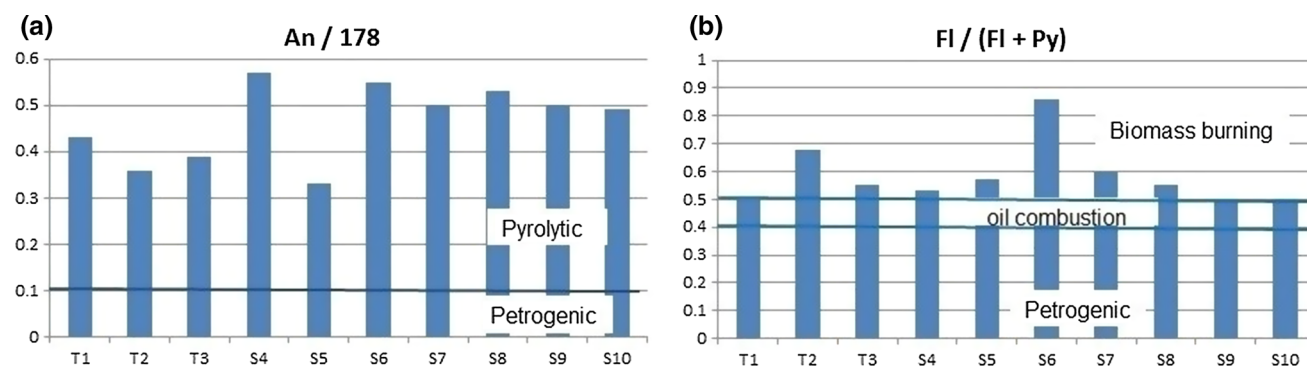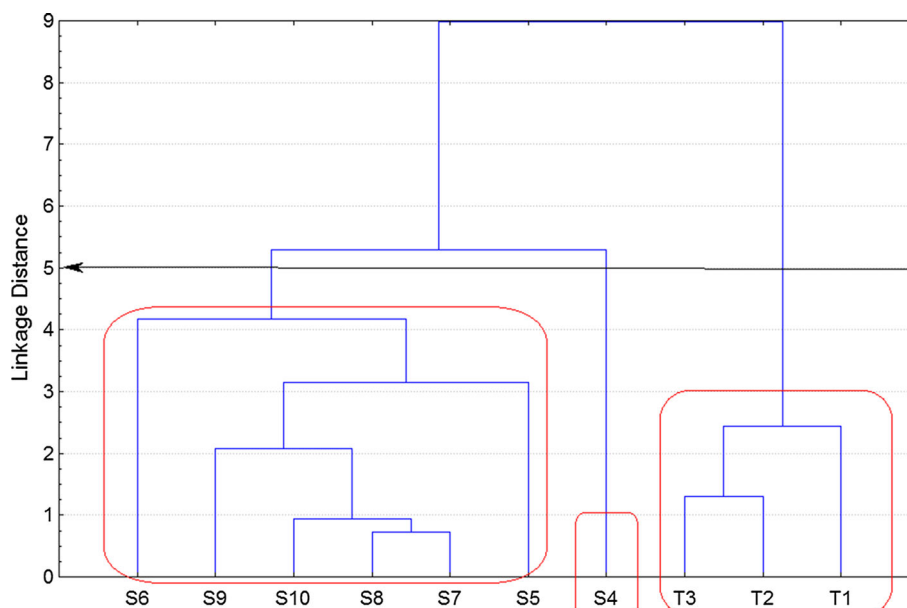
(a)

An / 178

Pyrolytic

Petrogenic

(b)

Fl / (Fl + Py)

Biomass burning

oil combustion

Petrogenic

Fig. 5 Plot of the ratios (a) An/178, (b) Fl/(Fl + Py)

Fig. 6 Dendrogram of hierarchical cluster analysis for all samples

lake). Third group was formed by the points sampled in the Solimões River with the greatest concentration of perylene and other biogenic compounds (Fig. 6).

Conclusions

The studied sediments were not considered polluted by fossil fuel and oil spilled since hopanes and steranes are from biogenic source or/and indicate bacterial contributions to the organic matter. A predominance of silt fractions is typical for modern fluvial deposits of the Solimões River. These deposits can most often be classified as silty and sandy silts, with a relatively low presence of clay. Additionally, the absence of UCM and the high concentrations of des-A-lupane (characteristic of angiosperms) are in accordance with uncontaminated sites characteristics. The C_{org}, TAR, CPI and C_{max} data observed for these sites

also lead to the same conclusions. Furthermore, some polycyclic aromatic hydrocarbons were identified in Coari Lake, but only at trace level; the PAH with the highest concentration is perylene indicating diagenetic conditions. PAH concentrations are well below the reference values for the concentrations of PAHs in freshwater sediments defined by ISQGs. The analysis of the An/178 and Fl/(Fl + Py) ratios, used to differentiate petrogenic from pyrolytic material, showed that these anthropogenic PAHs result from biomass burning. The $\delta^{13}C$ values of individual *n*-alkanes in the range C_{16}–C_{33} in the surface sediments vary between -35.0 and -23.1 ‰, suggesting an isotopic composition reflecting mainly C_3 plants and algae. The $\delta^{13}C$ values of individual *n*-alkanes in the range C_{16}–C_{25} showed biogenic and anthropogenic sources, and $\delta^{13}C$ values in the range C_{26}–C_{33} showed a biogenic source. The characterization of individual stable isotopic compositions ($\delta^{13}C$), aliphatic hydrocarbons and polycyclic aromatic

hydrocarbons in the Amazon region provides additional information for future environmental studies. No petrogenic contribution was found in the samples.

References

Almeida WS, Souza NM (2008) Coari: petroleum and sustainability—an Amazonian example. Desenv Meio Amb 17:69–92

Almeida WS, Souza NM (2010) A exploração petrolífera em Urucu (AM) e seus impactos na cobertura do solo. Informe Conjuntura & Informação – ANP 48:2-14

Bakhtiari AR, Zakaria MP, Yaziz MI, Lajis MNH, Bi X, Shafiee MRM, Sakari M (2010) Distribution of PAHs and *n*-alkanes in Klang River surface sediments, Malaysia. Pertanika J Sci Technol 18:167–179

Bícego MC, Weber RR, Ito RG (1996) Aromatic hydrocarbons on surface waters of admiralty bay, King George Island, Antarctica. Mar Pollut Bull 32:549–553

Boot CS, Ettwein VJ, Maslin MA, Weyhenmeyer CE, Pancost RD (2006) A 35,000 year record of terrigenous and marine lipids in Amazon fan sediments. Org Geochem 37:208–219

Canadian Council of Ministers of the Environment (2001) Canadian sediment quality guidelines for the protection of aquatic life: Introduction. Updated. In: Canadian environmental quality guidelines, 1999. Canadian Council of Ministers of the Environment, Winnipeg http://www.ccme.ca/en/resources/canadian_environmental_quality_guidelines/index.html

Castro IX, Silva JC, Rivas AAF, Freitas CEC (2008) PIATAM—Inteligência socioambiental estratégica na Amazônia: Governança gerando ciência & tecnologia. T&C Amazônian 15:52–58

Cox R, Lowe DR (1996) Quantification of the effects of secondary matrix on the analysis of sandstone composition, and a petrographic-chemical technique for retrieving original framework grain modes of altered sandstones. J Sediment Res 66:548–558

Decker J, Helmond KP (1985) The effect of grain size on detrital modes: a test of the Gazzi-Dickinson point-counting method-discussion. J Sediment Petrol 55:619

Didyk BM, Simoneit BRT, Brassell SC, Eglinton G (1978) Organic geochemical indicators of palaeoenvironmental conditions of sedimentation. Nature 272:216–222

Elias VO, Cardoso JN, Simoneit BRT (1996) Sesquiterpenoids in Amazon shelf waters. Org Geochem 25:241–250

Elias VO, Cardoso JN, Simoneit BRT (2000) Acyclic lipids in Amazon shelf waters. Estuar Coast Shelf Sci 50:231–243

Folk RL (1968) Petrology of sedimentary rocks. Hemphill's, Austin, pp 1–168

Foster IDL, Charlesworth SM (1996) Heavy minerals in the hydrological cycle: trends and explanations. Hydrol Process 10:227–261

Freitas CEC, Rivas AAF (2003) Data collection to risk assessment of the fluvial transportation of oil and natural gas in the Amazon Basin—PIATAM-Project. T Ecol Environ 60:271–278

Galka M, Apolinarska K (2014) Climate change, vegetation development, and lake level fluctuations in Lake Purwin (NE Poland) during the last 8600 cal. BP based on a high-resolution plant macrofossil record and stable isotope data (δ^{13}C and δ^{18}O). Quat Int 328–329:213–225

Gogou A, Bouloubassi I, Stephanou EG (2000) Marine organic geochemistry of the Eastern Mediterranean: 1. Aliphatic and polyaromatic hydrocarbons in Cretan Sea surficial sediments. Mar Chem 68:265–282

Gomes AO, Azevedo DA (2003) Aliphatic and aromatic hydrocarbons in tropical recent sediments of Campos dos Goytacazes, RJ, Brazil. J Braz Chem Soc 14:358–368

Green G, Nichols PD (1995) Hydrocarbons and sterols in marine sediments and soils at Davis Station, Antarctica: a survey for human-derived contaminants. Antarct Sci 7:137–144

Havelcováa M, Melegy A, Rapant S (2014) Geochemical distribution of polycyclic aromatic hydrocarbons in soils and sediments of El-Tabbin, Egypt. Chemosphere 95:63–74

Horowitz AJ, Elrick KA, Cook RB (1993) Effect of mining and related activities on the sediment trace element geochemistry of lake Coeur d'Alene, Idaho, USA, Part I: surface processes. Hydrol Process 7:403–423

IBGE 2015 http://cidades.ibge.gov.br/xtras/perfil.php?codmun=130120. Accessed in June, 2015

Instituto Nacional de Metrologia, Normalização e Qualidade Industrial (INMETRO) (2003) Orientações sobre Validação de Métodos de Ensaios Químicos, DOQ-CGCRE-008 http://www.inmetro.gov.br/Sidoq/Arquivos/CGCRE/DOQ/DOQ-CGCRE-8_02.pdf

International Conference on Harmonisation (ICH) (1995) Validation of analytical procedures: methodology, Q2B (CPMP/ICH/281/95) http://www.ich.org/fileadmin/Public_Web_Site/ICH_Products/Guidelines/Quality/Q2_R1/Step4/Q2_R1__Guideline.pdf

Ishiwatari R, Uzaki M, Yamada K (1994) Carbon isotope composition of individual *n*-alkanes in recent sediments. Org Geochem 21:801–808

Kennicutt MC II, Barker C, Brooks JM, De Freitas DA, Zhu GH (1987) Selected organic matter source indicators in the Orinoco, Nile and Changjiang deltas. Org Geochem 11:41–51

Laflamme RE, Hites RA (1978) The global distribution of polycyclic aromatic hydrocarbons in recent sediments. Geochim Cosmochim Acta 42:289–303

Magny M (2004) Holocene climate variability as reflected by mid-European lake-level fluctuations and its probable impact on pre historic human settlements. Quat Int 113:65–79

Maioli OLG, Oliveira CR, Dal Sasso MA, Madureira LAS, Azevedo DA, Aquino Neto FR (2012) Evaluation of the organic matter sources using the δ^{13}C composition of individual *n*-alkanes in sediments from Brazilian estuarine systems by GC/C/IRMS. Estuar Coast Shelf Sci 114:140–147

Martins CC, Bícego MC, Figueira RCL, Angelli JLF, Combi T, Gallice WC, Mansur AV, Nardes E, Rocha ML, Wisnisski E, Ceschim LMM, Ribeiro AP (2012) Multi-molecular markers and metals as tracers of organic matter inputs and contamination status from an environmental protection area in the SW Atlantic (Laranjeiras Bay, Brazil). Sci Total Environ 417–418:158–168

Matos FB, Camacho JR, Rodrigues P, Guimarães SC Jr (2011) A research on the use of energy resources in the Amazon. Renew Sustain Energy Rev 15:3196–3206

Meyers PA (2003) Applications of organic geochemistry to paleolimnological reconstructions: a summary of examples from the Laurentian Great Lakes. Org Geochem 34:261–289

Moita Neto JM, Moita GC (1998) Uma Introdução à análise exploratória de dados multivariados. Quim Nova 20:467–469

Muniz P, Pires-Vanin AMS, Mertins CC, Montone RC, Bícego MC (2006) Trace metals and organic compounds in the benthic environment of a subtropical embayment (Ubatuba Bay, Brazil). Mar Pollut Bull 52:1090–1117

Nehyba S, Hilscherová K, Jarkovsky J, Dusek L, Kuchovský T, Zeman J, Klánová J, Holoubek I (2010) Grain size, geochemistry

and organic pollutants in modern fluvial deposits in eastern Moravia (Czech Republic). Environ Earth Sci 60:591–602

Nesbitt HW, Young GM, McLennana SM, Keays RR (1996) Effects of chemical weathering and sorting on the petrogenesis of siliciclastic sediments, with implications for provenance studies. J Geol 104:525–542

Otto A, Simoneit BRT, Rember WC (2005) Conifer and angiosperm biomarkers in clay sediments and fossil plants from the Miocene Clarkia Formation, Idaho, USA. Org Geochem 36:907–922

Owens PN, Batalla RJ, Collins AJ, Gomez B, Hicks DM, Horowitz AJ, Kondolf GM, Marden M, Page MJ, Peacock DH, Petticrew EL, Salomons W, Trustrum NA (2005) Fine-grained sediment in river systems: environmental significance and management issues. River Res Appl 21:693–717

Pancost RD, Boot CS (2004) The palaeoclimatic utility of terrestrial biomarkers in marine sediments. Mar Chem 92:239–261

Pearson A, Eglinton T (2000) The origin of n-alkanes in Santa Monica Basin surface sediment: a model based on compound-specific $\Delta^{14}C$ and $\delta^{13}C$ data. Org Geochem 31:1103–1116

Peters KE, Walter CC, Moldowan JM (2005) The Biomarker Guide. Biomarkers and isotopes in the environment and human history, v. 1, 2nd edn. Cambridge University Press, Cambridge

Philp RP (1985) Fossil fuel biomarkers, applications and spectra. Elsevier, New York

Reddy C, Eglinton T, Palic R, Benitez-Nelson B, Stojanovic G, Palic I, Djordjevic S, Eglinton G (2000) Even carbon number predominance of plant wax n-alkanes: a correction. Org Geochem 31:331–336

Rogge WF, Medeiros PM, Simoneit BRT (2007) Organic marker compounds in surface soils of crop fields from the San Joaquin Valley fugitive dust characterization study. Atmos Environ 41:8183–8204

Rohmer M (1987) The hopanoids, prokaryotic triterpenoids and sterol surrogates. In: Schriner E, et al (eds) Surface structures of microorganisms and their interactions with the mammalian host, VCH Publishing, Weinlein, Germany

Rontani JF, Combe I, Giral PJP (1990) Abiotic degradation of free phytol in the water column: a new pathway for the production of acyclic isoprenoids in the marine environment. Geochim Cosmochim Acta 54:1307–1313

Roser BP, Korsch RJ (1986) Determination of tectonic setting of sandstone-mudstone suites using SiO_2 content and K_2O/Na_2O ratio. J Geol 94:635–650

Salem DMSA, Morsy FAM, El-Nemr A, El-Sikaily Khaled A (2014) The monitoring and risk assessment of aliphatic and aromatic hydrocarbons in sediments of the Red Sea, Egypt. Egypt J Aquat Res 40:333–348

Santos CYM, Azevedo DA, Aquino Neto FR (2004) Atmospheric distribution of organic compounds from urban areas near a coal-fired power station. Atmos Environ 38:1247–1257

Sikes EL, Uhle ME, Nodder SD, Howard ME (2009) Sources of organic matter in a coastal marine environment: evidence from n-alkanes and their $\delta^{13}C$ distributions in the Hauraki Gulf, New Zealand. Mar Chem 113:149–163

Silliman JE, Meyers PA, Eadie BJ (1998) Perylene: an indicator of alteration processes or precursor materials? Org Geochem 29:1737–1744

Silva TF, Azevedo DA, Aquino Neto FR (2007) Distribution of polycyclic aromatic hydrocarbons in surface sediments and waters from Guanabara Bay, Rio de Janeiro, Brazil. J Braz Chem Soc 18:628–637

Silva LSV, Piovano EL, Azevedo DA, Aquino Neto FR (2008) Quantitative evaluation of sedimentary organic matter from Laguna Mar Chiquita, Argentina. Org Geochem 39:450–464

Silva TR, Lopes SRP, Spörl G, Knoppers BA, Azevedo DA (2013) Evaluation of anthropogenic inputs of hydrocarbons in sediment cores from a tropical Brazilian estuarine system. Microchem J 109:178–188

Simoneit BRT (1977) Organic matter in eolian dusts over the Atlantic Ocean. Mar Chem 5:443–464

Statsoft program (2013) available in http://www.statsoft.com.br/

Stone PM, Walling DE (1996) The particle size selectivity of sediment mobilization for Devon Hill slopes. In: Anderson MG, Brooks SM (eds) Advances in hillslope hydrology. Willey, Chester, pp 507–527

Texeira CC, Siqueira CYS, Aquino Neto Fr, Miranda FP, Cerqueira JR, Vasconcelos AO, Landau L, Herrera M, Bannermaman K (2014) Source identification of sea surface oil with geochemical data in Cantarell, Mexico. Microchem J 117:202–213

Tolosa I, Bayona JM, Albaigés J (1996) Aliphatic and polycyclic aromatic hydrocarbons and sulfur/oxygen derivatives in north-western Mediterranean sediments: spatial and temporal variability, fluxes, and budgets. Environ Sci Technol 30:2495–2503

Tolosa I, Mora S, Sheikholeslami MR, Villeneuve J, Bartocci J, Cattini C (2004) Aliphatic and aromatic hydrocarbons in coastal Caspian Sea sediments. Mar Pollut Bull 48:44–60

Walling DE, Owens PN, Waterfall BD, Leeks GJL, Wass PD (2000) The particle size characteristics of fluvial suspended sediment in the Humber and Tweed catchments, UK. Sci Total Environ 251:205–222

Wang Z, Fingas M, Page DS (1999) Oil spill identification. J Chromatogr A 843:369–411

Wang Y, Yang H, Chen X, Zhang J, Ou J, Xie B, Huang C (2013) Molecular biomarkers for sources of organic matter in lacustrine sediments in a subtropical lake in China. Environ Pollut 176:284–291

Whitmore GP, Crook KAW, Johnson DP (2004) Grain size control of mineralogy and geochemistry in modern river sediment, New Guinea collision, Papua New Guinea. Sediment Geol 171:129–157